ELSEVIER

Biochimica et Biophysica Acta 1321 (1997) 79–92

BIOCHIMICA ET BIOPHYSICA ACTA
BBA

Structural and functional analysis of deficient mutants in subunit I of cytochrome *c* oxidase from *Saccharomyces cerevisiae*

Claus Ortwein [a], Thomas A. Link [a], Brigitte Meunier [b,1], Anne-Marie Colson-Corbisier [c], Peter R. Rich[1] [b], Ulrich Brandt [a,*]

[a] *Universitätsklinikum Frankfurt, Zentrum der Biologischen Chemie, Theodor-Stern-Kai 7, Haus 25B, 60590 Frankfurt am Main, Germany*

[b] *Glynn Research Institute, Glynn Bodmin, Cornwall PL30 4AU, United Kingdom*

[c] *Unité de Génétique, Université Catholique de Louvain, 1348 Louvain la Neuve, Belgium*

Received 7 March 1997; accepted 20 March 1997

Abstract

Four point mutations in subunit I of cytochrome *c* oxidase from *Saccharomyces cerevisiae* that had been selected for respiratory incompetence but still contained spectrally detectable haem aa_3 were analysed. The isolated mutant enzymes exhibited minor band shifts in their optical spectra and contained all eleven subunits. However, steady state activities were only a few percent compared to wild type enzyme. Using a comprehensive experimental approach, we first checked the integrity of the enzyme preparations and then identified the specific functional defect. The results are discussed using information from the recently solved structures of cytochrome *c* oxidase at 2.8 Å. Mutation I67N is positioned between haem *a* and a conserved glutamate residue (E243). It caused a distortion of the EPR signal of haem *a* and shifted its midpoint potential by 54 mV to the negative. The high-resolution structure suggests that the primary reason for the low activity of the mutant enzyme could be that asparagine in position 67 might form a stable hydrogen bond to E243, which is part of a proposed proton channel. Cytochrome *c* oxidase isolated from mutant T316K did not meet our criteria for homogeneity and was therefore omitted from further analysis. Mutants G352V and V380M exhibited an impairment of electron transfer from haem *a* to a_3 and ligand binding to the binuclear centre was affected. In mutant V380M also the midpoint potential of Cu_B was shifted by 65 mV to the positive. The results indicated for these two mutants changes primarily associated with the binuclear centre, possibly associated with an interference in the routes and/or sites of protonation which are required for stable formation of the catalytic intermediates. This interpretation is discussed in the light of the high resolution structure. © 1997 Elsevier Science B.V.

Keywords: Yeast; Cytochrome *c* oxidase; Random mutagenesis; Kinetics; Ligand binding

Abbreviations: EPR, electron paramagnetic resonance; PMSF, phenylmethylsulfonylfluoride; PMS, phenazine methosulphate; DCPIP, 2,6-dichlorophenolindophenol; DAD, 2,3,5,6-tetramethylphenylene diamine; FIRE, flash-induced reduction.

* Corresponding author. Fax: +49 69 6301 6970; E-mail: brandt@zbc.klinik.uni-frankfurt.de

[1] Present address: Department of Biology, University College London, Gower Street, London WC1E 6BT, United Kingdom.

PII S0005-2728(97)00035-2

1. Introduction

Cytochrome *c* oxidase (E.C. 1.9.3.1) is the terminal enzyme of the mitochondrial respiratory chain catalysing reduction of oxygen to water. It is a member of a large family of haem/copper containing protonmotive oxidases [1]. Yeast cytochrome *c* oxidase is composed of 11 different subunits and its kinetic and spectral properties have been characterised in detail [2]. The enzyme contains four redox-active metal-centres: Cu_A, low-spin haem *a*, high-spin haem a_3 and Cu_B. Haem a_3 and Cu_B are coordinated by subunit I and form the binuclear centre which is the oxygen reduction site. Recently the high resolution structures of cytochrome *c* oxidases from *Paracoccus denitrificans* and from bovine heart enzyme obtained by X-ray crystallography were published [3,4]. These structures represent a basis for understanding the mechanisms of proton translocation and electron transport at a molecular level.

Since the yeast *Saccharomyces cerevisiae* can grow fermentatively even if the respiratory chain is inactive, this organism is well suited to analyse mutants deficient in cytochrome *c* oxidase. Here we describe a comprehensive approach to identify functional changes induced by four randomly selected mutations in subunit I of yeast cytochrome *c* oxidase in the vicinity of the haem groups. Taking advantage of the high degree of conservation of the catalytic subunits between the bacterial and the mitochondrial enzyme [3,4], we interpreted our results in the light of the high-resolution structure available for *P. denitrificans*.

2. Materials and methods

Technical yeast extract was obtained from Ohly, Hamburg (Germany). Difference spectra were recorded on a Bruins Omega-10 spectrophotometer or by sequential scanning of the same sample with a single beam instrument built in-house (Glynn Research Institute). Cytochrome *c* oxidase concentration was determined by reduced minus oxidised spectra at room temperature using an extinction coefficient of 24 $mM^{-1} \cdot cm^{-1}$ at 603–630 nm. EPR[1] spectra were recorded on a Bruker 200D X-band spectrometer equipped with cryogenics, peripheral equipment and data-acquisition/manipulation facilities as described previously [5]. Protein concentration was determined using a modified Lowry protocol [6]. The metal content was determined by Dr. Guy Steffens (Aachen, Germany) using Inductively Coupled Plasma-Atom Emission Spectroscopy as described in [7]. Structural simulations and calculations of the preferred rotamers were carried out using program O [8].

2.1. Strains, media and preparation of mitochondrial membranes

For the isolation of wild type enzyme, *Saccharomyces cerevisiae* strain KM91 was cultivated in 2% yeast extract, 3% DL-lactate at 30°C and harvested at early stationary phase. The mutant strains L174 (I67N), L29 (T316K), L53 (G352V) and L318 (V380M) which all carry a single amino acid exchange in the mitochondrially coded subunit I of cytochrome *c* oxidase were selected and characterised by the methods of Meunier et al. [9] and Brown et al. [10]. The mutants, which will be denoted by their amino acid exchange in the following, grew very poorly on glycerol medium and were cultivated on agar plates in YGal medium (1% yeast extract KAT technical, 3% galactose) or for revertant check in N3 medium (1% yeast extract KAT technical, 3% glycerol). After collecting the cells and suspending in 300 mM sorbitol, 5 mM EDTA, 50 mM potassium phosphate, pH 7.3 and 1 mM PMSF they were broken with glass-beads in a bead-mill (Biospec products, Bartlesville, USA). Cell debris was removed by centrifugation at 3500 *g* for 15 min and mitochondrial membranes were obtained by a second centrifugation step at 30,000 *g* for 1 h.

2.2. Purification of cytochrome c oxidase

Purification of wild type cytochrome *c* oxidase in the presence of chloride was performed as described previously [2]. For the isolation of the mutant enzymes not the first but the second hydroxylapatite column was loaded in batch and was equilibrated with 50 mM rather than 70 mM sodium phosphate. Subsequent blue-native gelelectrophoresis [11] followed by tricine-SDS-PAGE [12] was carried out to determine the subunit composition of the protein

complexes. Concentrated oxidase (> 40 μM) was stored in liquid nitrogen after addition of 10% (w/v) glycerol.

2.3. Catalytic activity

Catalytic turnover was determined spectrophotometrically by oxidation of reduced cytochrome *c* according to Brandt et al. [13] in 120 mM NaCl, 1 mM EDTA, 20 mM K^+/Hepes pH 7.4, 0.05% dodecyl maltoside at 25°C. Final concentrations of 5–50 nM enzyme and 0.5–50 μM substrate were used. Maximal turnover numbers (k_{cat}) and K_m values were calculated by fitting the data to the Michaelis–Menten equation using the Marquardt algorithm [14].

2.4. Cyanide-binding to oxidised enzyme

Kinetics using 2 μM cytochrome *c* oxidase in 0.05% dodecyl maltoside, 60 mM Na_2SO_4, 1 mM EDTA, 20 mM K^+/Hepes pH 7.4 and 20 mM KCN were recorded at 434 nm–411 nm on a Perkin-Elmer dual-wavelength spectrophotometer attached to a Compaq Deskpro personal computer as described in [13]. The traces were fitted for 1–3 exponentials using the Marquardt algorithm [14].

2.5. Laser flash photolysis

Cyanide and carbon monoxide were photolysed from the fully reduced, ligated forms of purified enzyme with a frequency-doubled Nd/YAG laser (Spectron Physics) which produced a 10 ns flash at 532 nm with an energy in excess of 100 mJ/flash. Photolysis and subsequent kinetics of rebinding were monitored at 430–445 nm for carbon monoxide or 592–610 nm for cyanide. Transients were recorded cyclically and signal averaged ten times at each wavelength, as described in [15,16].

Recombination rates of cyanide at various cyanide concentrations could be used to determine the rate constants (k_{on} and k_{off}) and the dissociation constant (K_d) from a plot of apparent rate constant, k_{obs}, versus cyanide concentration [16,17]. An independent measurement of the K_d was also obtained by titration of the magnitude of the cyanide binding spectrum with successive additions of cyanide to the reduced enzyme.

2.6. Potentiometric titrations

Anaerobic redox titrations of cyanide-ligated oxidase were carried out in 1.3 ml of 150 mM Na^+/Hepes, 150 mM NaCl, 0.05% dodecyl maltoside, 200 U/ml catalase and 50 U/ml superoxide dismutase, all at pH 7.5. Purified cytochrome *c* oxidase was added to around 3 μM and the mixture was kept anaerobic with a positive pressure of argon above the liquid surface. Redox mediators were (E_m, concentration): PMS (phenazine methosulphate) +80 mV, 8 μM; DCPIP (2,6-dichlorophenolindophenol) +220 mV, 15 μM; DAD (2,3,5,6-tetramethylphenylene diamine) +275 mV, 50 μM; ferricyanide +440 mV, 50 μM; 1,2-naphthoquinone-4-sulphonate +215 mV, 5 μM; 1,2-naphthoquinone +143 mV, 5 μM; 1,4-benzoquinone +293 mV, 50 μM; 2,6-dimethyl-1,4-benzoquinone +168 mV, 40 μM; methyl-hydroquinone +224 mV, 40 μM; cytochrome *c* +255 mV, 3 μM. Potassium ascorbate (20 mM stock solution, pH 7.5) was used as reductant and potassium permanganate (10 mM stock solution, pH 7.5) was used as oxidant. Redox potentials were measured in stirred samples with a polished glassy carbon electrode and a Ag/AgCl reference electrode, as described in [18,19]. At each potential, stirring was stopped and spectra were taken from 390 to 490 nm. Potential was recorded at the start and the end of the scans and absorbance changes were plotted versus the average of the two potential readings. The reduction of haem *a* was monitored by a triple wavelength measurement at $445-(435+455)/2$ nm and the reduction of cytochrome *c* was monitored at $418-(410+426)/2$ nm. These triple wavelength measurements minimised interference from redox dyes or baseline drift.

2.7. Reaction of the fully reduced enzyme with oxygen

The kinetics of reaction of fully reduced cytochrome *c* oxidase with oxygen at room temperature were monitored by the flow/flash method as described in [20,21]. Purified cytochrome *c* oxidase was dissolved to around 0.8 μM in 0.5 ml of 50 mM potassium phosphate, 0.5 mM EDTA, 0.05% dodecyl maltoside, 200 U/ml catalase, 50 U/ml superoxide dismutase, 10 mM ascorbate, 1 μM PMS, and 0.2 μM cytochrome *c* at pH 8. Samples were saturated

with CO, placed in a sealed cuvette, and left at room temperature for several minutes until the fully reduced, CO-ligated form had been generated. This was confirmed by monitoring the size of the CO-induced binding spectrum in the Soret region. 0.15 ml of air-saturated buffer was then injected into the solution and reaction with oxygen was initiated by laser flash photolysis of the CO compound. The kinetics of reaction between unligated enzyme and oxygen were monitored at 445 nm.

2.8. Single electron distribution in the enzyme by FIRE

The reaction of ferrocytochrome *c* with fully oxidised cytochrome *c* oxidase in the 0–200 ms time range was monitored by the FIRE method essentially as described in [22]. Purified enzyme was dissolved aerobically to around 0.7 μM in 0.5 ml of 50 mM potassium phosphate, 0.5 mM EDTA, 0.05% dodecyl maltoside, 200 U/ml catalase, 50 U/ml superoxide dismutase, 10 μM oxidised cytochrome *c* and 60 μM PMS, all at pH 8 in the presence of only a trace catalytic amount of bovine cytochrome *c* oxidase to allow the slow reoxidation of ferrocytochrome *c* in the dark period between flashes. Photoreduction of cytochrome *c* was initiated with a xenon flash (20 joules capacitance; 6 μs half peak width; Glynn Research Enterprises, Bodmin, UK) filtered with short pass filters to produce a blue flash actinic for the PMS/EDTA photosystem [22]. This initiated a rapid reduction of ferricytochrome *c* by reduced PMS, followed by a reaction between ferrocytochrome *c* and oxidase. The same sample could be used repeatedly at many individual wavelengths by allowing a dark-adaptation of at least 15 s between flashes, during which time the system reverted to the fully oxidised state by reaction with oxygen. The redox changes of cytochrome *c* and cytochrome *c* oxidase were plotted as $550-(544+556)/2$ nm ($\epsilon = 14.7$ $mM^{-1}\cdot cm^{-1}$, [23]) and $603-(593+613)/2$ nm ($\epsilon = 14$ $mM^{-1}\cdot cm^{-1}$), respectively.

A typical experiment is shown in Fig. 1: From the timecourse of cytochrome *c* reduction (trace A) we could estimate a yield of ferrocytochrome *c*/flash of 0.64 μM. This corresponds to approx. 1 electron per oxidase. This ratio of reductant/oxidase meant that the majority of oxidases would receive only a single

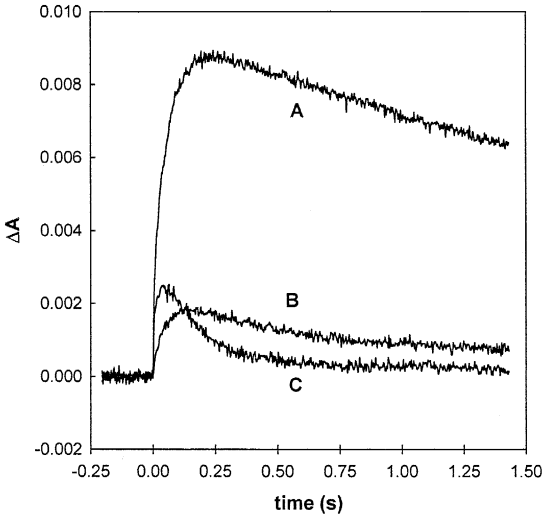

Fig. 1. The reaction of ferrocytochrome *c* with oxidised cytochrome *c* oxidase. The reaction of ferrocytochrome *c* with fully oxidised cytochrome *c* oxidase were monitored by the FIRE method. Purified enzyme was dissolved to around 0.7 μM in 0.5 ml of 50 mM potassium phosphate, 0.5 mM EDTA, 0.05% dodecyl maltoside, 200 U/ml catalase, 50 U/ml superoxide dismutase, 10 μM oxidised cytochrome *c* and 60 μM PMS, all at pH 8. A xenon flash initiated a rapid reduction of ferricytochrome *c* by reduced PMS, followed by the reaction between ferrocytochrome *c* and oxidase. Trace A, reduction of cytochrome *c* initiated by FIRE in absence of yeast cytochrome *c* oxidase. A catalytic amount of bovine cytochrome *c* oxidase (0.04 μM) was added in the cuvette to allow the re-oxidation of ferrocytochrome *c*. Reduction of cytochrome *c* was monitored at $550-(544+556)/2$ nm. Quantitation of ferrocytochrome *c* produced per flash was obtained using $\epsilon = 14.7$ $mM^{-1}\cdot cm^{-1}$. Traces B and C, 0.7 μM wild type yeast cytochrome *c* oxidase was added in the cuvette. Photoreduction of cytochrome *c* was initiated as before and was followed by the reaction between ferrocytochrome *c* and oxidase. Trace B: reduction of haem *a* by ferrocytochrome *c* was monitored at $603-(593+613)/2$ nm. $\epsilon = 14$ $mM^{-1}\cdot cm^{-1}$ was used for the quantitation of haem *a*. Trace C: reduction and re-oxidation of cytochrome *c* was monitored at $550-(544+556)/2$ nm.

electron during the reduction phase, a point confirmed by the fact that essentially the same results were obtained when the yield of ferrocytochrome *c* was lowered to 0.2 μM/flash by reducing the flash intensity (data not shown). After this quantitation of the yield of ferrocytochrome *c* per flash, yeast cytochrome *c* oxidase was added to the same sample and the photoreduction was repeated. The yield of reducing equivalents/flash was unchanged after this addition (data not shown). However, in this case the

ferrocytochrome *c* rapidly reduced the yeast oxidase so that an equilibrium mixture of ferro/ferricytochrome *c* and singly-reduced oxidase was formed in 100–200 ms, the rate being limited by the oxidation of photoreductant by ferricytochrome *c*. This was followed by a slower redistribution of electrons between oxidases, ultimately to be reoxidised by oxygen (catalysed by the cytochrome *c*). Hence, the cytochrome *c* and the oxidase return to the fully oxidised state in the dark and can be photoactivated again. The behaviour of cytochrome *c* and haem *a* in the wild-type enzyme is shown in Fig. 1, traces B and C.

From the difference between the ferrocytochrome *c* reduction level in trace A and its reduction level in trace C, we determined how many electrons have entered the oxidase at any given time and, from trace B, estimate how many of them have appeared on haem *a*. The difference between the total number of electrons donated by cytochrome *c* and the number electrons appearing on haem *a* gives the number that have been transferred to the binuclear centre. From this calculation, we were able to determine whether electron distribution between haem *a* and the binuclear centre was in accord with the equilibrium midpoint potentials of the individual redox centres.

3. Results

We analysed four mutants I67N, T316K, G352V and V380M that had been selected from a random mutagenesis approach [9]. The high resolution structures revealed that all four mutations are in close vicinity to either haem *a* or haem a_3. Mutations in residue T316 have been analysed previously in cytochrome *bo* from *Escherichia coli* [24,25], but for the remaining three positions no mutants have been reported so far. We developed a set of specific tests that allowed us to first test the structural integrity and homogeneity of enzyme prepared from the mutants and then to identify and analyse the functional defect.

3.1. Purification and general properties of the mutant enzymes

We first compared yield, purity and catalytic activity of mitochondrial membranes and isolated cytochrome *c* oxidase from the parental strain and mutants I67N, T316K, G352V and V380M (Table 1). The haem content of mitochondrial membranes from the respiratory deficient mutant strains was about half when compared to the parental strain (Table 1). This resulted in a correspondingly lower haem to protein ratio of the cytochrome *c* oxidase preparations. However, to avoid preparation artefacts no further attempts were made to remove the remaining impurities, as spectral analysis (see below) revealed no other haem containing proteins which might have interfered with the functional analysis. Possible global effects caused by the point mutations were excluded using several specific tests.

Blue-native-PAGE [11] of the enzyme preparation showed a number of proteins below 100 kDa but no

Table 1
Activity and yield of typical cytochrome *c* oxidase preparations

	Membranes			Purified enzyme							
	aa_3/protein	k_{cat}	λ_{max}	aa_3/protein	yield	K_M	k_{cat}	λ_{max}			metals
			redox					redox	oxid.	red.	Fe:Cu:Zn:Mg
	(nmol/mg)	(s^{-1})	(nm)	(nmol/mg)	(%)	(μM)	(s^{-1})	(nm)	(nm)	(nm)	
Parental	0.20	1500	603	4.4	30	18	1380	603	424	444	2.0:3.0:1.5:0.9
I67N	0.09	59	602	1.6	28	6.5	25	601	426	444	2.3:2.7:1.9:1.3
T316K	0.07	41	602	3.1	22	1.3	22	603	426	441	2.1:3.0:1.5:1.4
G352V	0.07	34	602	2.0	14	2.5	22	600	425	442	2.1:2.9:1.6:0.7
V380M	0.11	86	604	2.4	18	5.6	84	605	423	445	n.d.

Michaelis–Menten parameters were determined as described in Section 2. Yields are given as percent haem aa_3 with mitochondrial membrane set at 100%. The two 'redox' labelled wavelength give the α-band absorption maxima of dithionite reduced-ferricyanide oxidised difference spectra from mitochondrial membranes and purified enzyme. The γ-band maxima of the air-oxidised and dithionite reduced enzymes are given. The metals were determined by ICP-AES and normalised by setting iron + copper to 5.0 atoms per oxidase [7]. n.d., not determined.

partially assembled cytochrome *c* oxidase. The following tricine-SDS-PAGE [12] revealed that the subunit compositions of all enzyme preparations was indistinguishable from the wild-type enzyme indicating full assembly of all four mutant enzymes (data not shown). Also the fact that the iron to copper ratio was not altered significantly (Table 1), seems to exclude specific loss of one of the prosthetic groups in any of the mutants tested. Based on the EPR-spectra of Cu_A and functional analysis of the binuclear centre (see below), we concluded that this also holds for I67N, which exhibited a somewhat lower relative copper content.

The steady-state activity of cytochrome *c* oxidase isolated from the different mutant strains, were between 2 and 6% of the parental strain (Table 1). Comparison of maximal turnover numbers determined for mitochondrial membranes and purified oxidase indicated that no significant loss of activity occurred during isolation of the mutant enzymes. The K_M values of the mutant enzymes were 3–14-fold lower than for the wild-type which partly reflected the much lower k_{cat}. More detailed analysis of the electron transfer into cytochrome *c* oxidase (see below) suggested that another factor responsible for lower K_M values was a significant contribution of re-reduction of cytochrome *c* due to higher steady-state levels of reduced Cu_A in the mutant enzymes, but that the rate of reduction by ferrocytochrome *c* was normal in all four mutants. Therefore, these rather small differences in the K_M values did not indicate any significant modifications of the cytochrome *c* binding site by the point mutations analyzed here.

The optical spectra of cytochrome *c* oxidase purified from the mutant strains revealed some minor differences when compared to wild type (Table 1). In all cases, the observed shifts of the α-band maxima appeared not to be caused by the isolation procedure, although they were somewhat more pronounced in purified enzyme than in mitochondrial membranes (cf. Table 1).

Cyanide binding to the oxidised enzyme was analysed to test for heterogeneity of the binuclear centre, which can be caused by the isolation procedure [26,13]. Enzyme isolated from mutants I67N and G352V showed biphasic, but largely fast kinetics (Table 2). With mutant V380M a high portion of slow cyanide binding was observed, but complete reduction and reoxidation brought it back to 85% fast phase (data not shown). This indicated only a minor heterogeneity that was reversible and limited to the ligand state of the binuclear centre.

Three exponentials were necessary to fit the kinetics of cyanide binding to the oxidised enzyme from mutant T316K of which only 47% were fast phase. The occurrence of a third phase and the fact that the enzyme could not be reverted by reduction/reoxidation to a largely fast form indicated a much more severe heterogeneity of enzyme from T316K that was not limited to the ligand state of the binuclear centre. This suggested that this mutation had less well defined effects on the protein environment of the redox centres. It should also be noted that despite of a large fraction of slow enzyme in preparations from this mutant, a corresponding blue shift of the Soret-maxima for the oxidised enzymes ([2], cf. Table 1) was not observed.

Table 2
Cyanide binding kinetics

Strain	λ_{max}	Fast phase			Medium/slow phase		
	CN-ligated (nm)	$t_{1/2}$ (s)	k_{obs} (s^{-1})	(%)	$t_{1/2}$ (s)	k_{obs} (s^{-1})	(%)
Parental	428	5.2	0.13	93	147	0.005	7
I67N	430	1.7	0.41	66	70	0.010	34
T316K	428	0.9	0.77	47	7.9/148	0.088/0.005	18/35
G352V	428	1.2	0.58	75	37	0.019	25

Halftimes and observed kinetic constants of cyanide binding to the binuclear centre are listed. Kinetics were recorded over 10 min after addition of 20 mM neutralised KCN to 2 μM cytochrome *c* oxidase. The first column give the γ-band absorption maximum of the oxidised enzyme after cyanide incubation

In summary, all mutant enzymes had only a residual steady state activity, but were assembled correctly and contained all redox-centres in stoichiometric amounts. Mutant T316K revealed a marked and persistent heterogeneity of the binuclear centre (see below).

Following the assessment of the general properties of enzyme preparations, which revealed that only one of the mutations caused a significant heterogeneity, we performed a series of tests to identify the principal effects of the mutations. In the following the rationale behind these tests will be outlined in detail using the results obtained for mutant I67N.

3.2. I67N – a mutation near haem a

The mutated residue, isoleucine-67, is located in the second transmembrane helix of subunit I of yeast cytochrome *c* oxidase and is only five residues apart from histidine-62, one of the axial ligands of haem *a*.

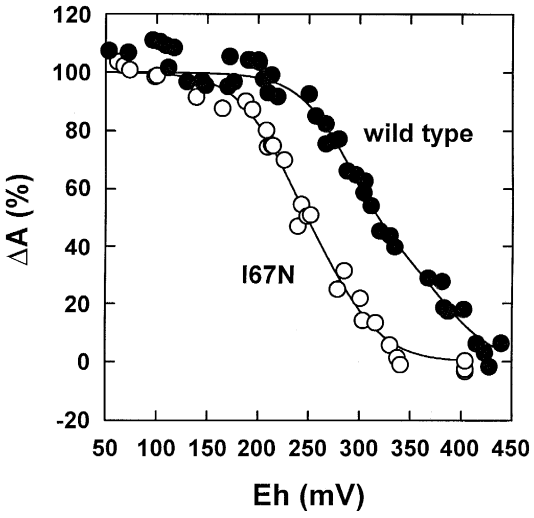

Fig. 2. Redox titration of cytochrome *c* oxidase. Anaerobic redox titrations in presence of 1.5 mM cyanide were carried out under argon in 1.3 ml of 150 mM Hepes, 150 mM NaCl, 0.05% dodecyl maltoside, 200 U/ml catalase and 50 U/ml superoxide dismutase, all at pH 7.5. Purified cytochrome *c* oxidase was added to around 3 μM. Redox mediators are described in Materials and Methods. At each potential, spectra were taken from 390 to 490 nm and absorbance changes versus potential were plotted. The reduction of haem *a* was monitored by a triple wavelength measurement at $445-(435+455)/2$ nm. Simulations of redox behaviour were calculated as described [27]. Symbols are: closed circles wild-type data; open circles, I67N data; simulations are shown as solid lines.

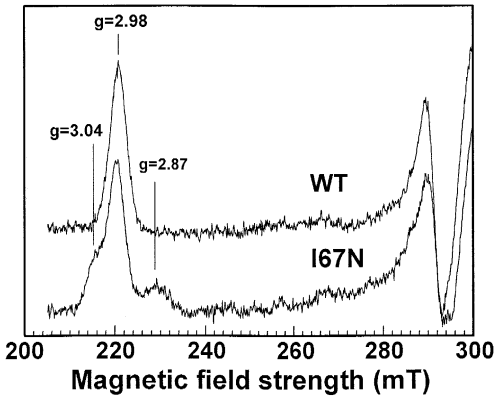

Fig. 3. EPR spectra of mutant I67N and wild type oxidase. EPR spectra of the low spin haem region of cytochrome *c* oxidase purified from the parental strain and mutant I67N are shown. The spectrum of the low spin haem *a* of the mutant shows a split band. The *g*-values are indicated by arrows. Enzyme concentrations were 37 μM and 44 μM for parental strain and mutant, respectively. The EPR conditions were as follows: microwave frequency, 9185 MHz; modulation frequency, 100 kHz; modulation amplitude, 1.6 mT; microwave power, 0.8 mW; temperature, 19 K.

In both 3D structures, it lies between haem *a* and the conserved glutamate, E243.

To analyse the state of the redox-centres, we determined their midpoint potentials and analysed their EPR-spectra: Fig. 2 shows redox titrations of the wild type enzyme and the mutant I67N. In the cyanide-ligated wild-type enzyme, the midpoint potential (E_m) of haem a_3 is lowered so that haem *a* can be titrated while haem a_3 remains oxidised. Under these conditions, haem *a* does not titrate as a classical '$n=1$' component [27], due to an anticooperative interaction between haem *a* and Cu_B [28–30]. Analysis of the shape of the titration curve can provide an estimate of the E_m of haem *a* and Cu_B (which is optically invisible), and the strength of their redox interaction. Simulations were made as described in [27], using a model for anticooperative interaction between haem *a* and Cu_B but without taking account of the weak interaction with Cu_A. For the wild type enzyme this analysis (Table 4) gave an E_m of 360 mV for haem *a* and 370 mV for Cu_B, with an anticooperative interaction between them of -60 mV. These values are similar to those found with the bovine enzyme [27,31]. In the mutant I67N, the E_m of haem *a* was 54 mV lower than the wild type, whereas the E_m of Cu_B and

the interaction between them was not affected. Other data from redox titrations of the unligated and formate-ligated enzyme confirmed this result and also showed that haem a_3 was not affected (data not shown).

Fig. 3 shows the haem *a* region of the EPR spectra of the enzyme from mutant I67N and the parental strain. While the Cu_A region was found to be unchanged (not shown), the low spin g_z signal of the mutant enzyme was split into three bands. This indicated a perturbation and heterogeneity in the haem *a* environment: EPR spectra of oxidised low-spin haems (d^5) reflect the distribution of the electron hole among the t_{2g} orbitals (d_{xy}, d_{xz}, d_{yz}) which depends on the axial and rhombic distortion of the octahedral ligand field of the iron atom. The g_z value of 2.98 found for the wild type and mutant enzyme is characteristic for a bis-histidine coordinated haem. The two additional g_z values (3.04 and 2.87) that were found for the mutant enzyme reflect the presence of additional substates with slightly different coordination geometries. However, the shifted g_z values are still indicative of bis-histidine coordination and indicate only subtle conformational changes in the haem-environment. Thus, the midpoint-potential and the EPR-lineshape for haem *a* was altered by mutation I67N, while the other redox-centres were unaffected.

As a test of the state of the channel(s) through which cyanide and carbon monoxide move and to check for protein heterogeneity, we analysed the kinetics of binding to the reduced enzyme for these ligands of the binuclear centre. In mutant I67N both rates were hardly affected (Table 3).

To test for changes in the electron transfer at the binuclear centre, the reaction of fully reduced oxidase with oxygen was monitored at 445 nm after laser photolysis of CO from the reduced enzyme in presence of oxygen (Fig. 4 and Table 5). The rate constants of 5500 and 1200 s^{-1} obtained with the wild-type enzyme at this wavelength are similar to the values of around 10^4 s^{-1} and 10^3 s^{-1} reported for the bovine enzyme, which have been attributed to the conversion of the peroxy to oxyferryl and oxyferryl to oxidised states, respectively. In our case, the two faster phases of binding of oxygen and formation of the peroxy compound were not resolved since we used only 60 μM oxygen, rather than the 1 mM used in [32,33]. Both rates and the ratio between them were almost identical for mutant I67N (Table 5), indicating that the mutation did not significantly affect oxygen chemistry at the binuclear centre.

To test whether electron distribution within cytochrome *c* oxidase was affected by the mutation, the kinetics of reaction of ferrocytochrome *c* with fully oxidised cytochrome *c* oxidase were monitored by the FIRE method (Flash-Induced chemical photoREduction) as described in the Section 2. For the wild type enzyme (Fig. 1, Table 6) at the point of maximal haem *a* reduction (0.15 seconds after the flash), 0.12 μM electrons (19% of the electrons produced per flash) remained on cytochrome *c* and 0.52 μM electrons had been donated to the oxidase. Of these

Table 3
Recombination kinetics of CO and cyanide after laser flash photolysis

	CO	CN^-			λ_{max}
	$k_{obs.}(s^{-1})$	$k_{on}(M^{-1} \cdot s^{-1})$	$k_{off}(s^{-1})$	K_d(mM)	CN-ligated(nm)
Parental	67	200	0.08	0.40	592
I67N	65	500	0.06	0.12	590
G352V	25	1000	0.12	0.12	590
V380M	72	30	0.03	1.00	591

Purified cytochrome *c* oxidase was dissolved to around 0.8 μM in 0.6 ml of 50 mM potassium phosphate, 0.5 mM EDTA, 0.05% dodecyl maltoside. pH 7. The sample was incubated with a small amount of dithionite until the enzyme had become fully reduced, and was then bubbled for 3 min with CO or treated with cyanide. Transients after photolysis at different wavelengths were recorded cyclically and signal averaged ten times at each wavelength. The observed rate constant (k_{obs}) was obtained by fitting an exponential decay to the transient at 430–445 nm for CO or 592–610 nm for cyanide. For cyanide, the experiment was repeated at several cyanide concentrations and k_{on}, k_{off} and K_d were determined from plots of k_{obs} versus cyanide concentration. The last column gives the maximum of the (reduced plus cyanide) minus reduced difference spectrum.

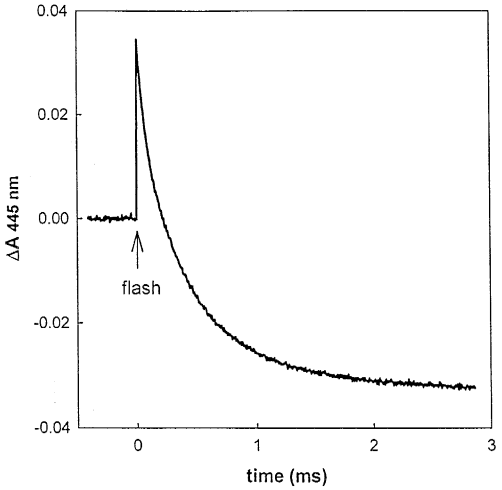

Fig. 4. Kinetics of reaction of fully reduced cytochrome *c* oxidase with oxygen. The kinetics of reaction of fully reduced cytochrome *c* oxidase with oxygen at room temperature were monitored by the flow/flash method. Purified cytochrome *c* oxidase was dissolved to around 0.8 μM in 0.5 ml of 50 mM potassium phosphate, 0.5 mM EDTA, 0.05% dodecyl maltoside, 200 U/ml catalase, 50 U/ml superoxide dismutase, 10 mM ascorbate, 1 μM PMS, and 0.2 μM cytochrome *c* at pH 8. The samples were saturated with CO and placed in a sealed cuvette. When the fully reduced, CO-ligated form had been fully generated, 0.15 ml of air-saturated buffer was injected into the solution and reaction with 60 μM oxygen was initiated by laser flash photolysis of the CO compound. The kinetics of reaction between unligated enzyme and oxygen were monitored at 445 nm. Rates of reaction were obtained by fitting exponential decays to the transient kinetic trace.

donated electrons, 23% were on haem *a* and, therefore, 77% should have been transferred to the binuclear centre. After the point of maximal haem *a* reduction, both haems *a* and *c* reoxidised as the P, F, and, finally, the fully oxidised forms of the oxidase were formed by a slower redistribution of the available electrons.

For enzyme from mutant I67N, the initial rate of reduction of haem *a* by cytochrome *c* was unaffected (Table 6). The rate of transfer from ferrocytochrome *c* to oxidase was therefore still much faster than the oxidation of photoreductant by ferricytochrome *c*, and that the electron donation rate into the enzyme could not account for its low turnover number. However, the peak level of reduction of haem *a* was altered. Only 11% of the electrons donated from ferrocytochrome *c* appeared on haem *a*. Hence, the missing 89% should have been transferred to the binuclear centre. This behaviour is consistent with the lower E_m of haem *a* indicated by redox titration and suggested that donation of a single electron into the binuclear centre was still quite feasible on this timescale.

3.3. Mutations near the oxygen reduction site

The residues changed in the remaining three mutants T316K, G352V and V380M are located in helix VIII, IX and X of subunit I, respectively, but are all in vicinity of the binuclear centre. For the analysis of these mutations, the same experimental approach as for mutation I67N was used, but in the following only the significant deviations from wild-type behaviour will be discussed in detail.

3.4. Mutant T316K

Mutant T316K displayed homogeneous kinetics of recombination of CO with $k_{obs} = 100\ s^{-1}$ whilst still in cells [10]. However, solubilisation by our standard method induces biphasicity in the carbon monoxide rebinding kinetics with k_{obs} values of 125 and 15 s^{-1}. Heterogeneity of these parameters in mutant forms of cytochrome bo_3 [15] indicates heterogeneous or unstable protein. This is consistent with the observed triphasic cyanide binding (cf. Table 2) to the oxidised enzyme (see above). Such persistent heterogeneity that is indicative of a poorly defined structural change around the binuclear centre presents a major obstacle for the interpretation of the more detailed tests and it is for this reason that mutant T316K was omitted from further analysis.

Table 4
Simulated E_m and redox interaction values from titration of the cyanide ligated forms of wild type and mutant cytochrome *c* oxidase

E_m	Parental	I67N	G352V	V380M
	(mV vs. SHE)			
Haem *a*	360	306	360	360
Cu_B	370	370	360	425
Interaction a/Cu_B	−60	−66	−60	−145

Values were obtained by simulation of the anaerobic titration data of the cyanide-ligated forms of the enzymes as described in Fig. 2. SHE, standard hydrogen electrode.

Table 5
Kinetics of reaction of fully reduced cytochrome *c* oxidase with oxygen

Strain	Fast phase $k_{obs}(s^{-1})$	Slow phase $k_{obs}(s^{-1})$	Fraction of slow phase
Parental	5500	1200	0.55
I67N	5800	1700	0.5
G352V	2900	650	0.8
V380M	5700	1270	0.5

Reaction of fully reduced cytochrome *c* oxidase with oxygen at room temperature was monitored by the flow/flash method as described in Fig. 4. Air-saturated buffer was injected into a solution containing fully reduced CO-ligated cytochrome *c* oxidase and reaction with oxygen was initiated by laser flash photolysis of the CO compound. The kinetics of reaction between unligated enzyme and oxygen were monitored at 445 nm. Rate constants were obtained by fitting biphasic exponential decays to the transients.

3.5. Mutant G352V

Ligand binding to the reduced binuclear centre of the purified enzyme from mutant G352V was altered. The recombination of carbon monoxide was slowed down from 67 s^{-1} to 25 s^{-1} while rebinding of cyanide to the reduced enzyme was accelerated 5-fold (Table 3).

Redox-titration in the presence of cyanide was similar to the wild-type, indicating that neither the E_m values of haem *a* nor Cu_B, nor their interaction, were affected. However, we were unable to titrate the unligated or formate-ligated forms of this enzyme, because loss of spectrally detectable haem during these titrations indicated some instability (data not shown). This observation is consistent with a structural displacement of the haem a_3-farnesyl chain by introduction of an isopropyl sidechain as suggested by an examination of the high resolution structure (see Discussion).

The reaction of the reduced enzyme with oxygen (Table 5) was slower by a factor of around two in comparison to wild-type. However, this is still much faster than its maximum turnover number and, therefore, cannot be the explanation for the low steady state turnover.

Single electron reduction by cytochrome *c* resulted in an accumulation on haem *a*, again at a rate too fast to account for the impaired turnover number, but with markedly decreased transfer to the binuclear centre in comparison to the wild-type enzyme (Table 6). This is likely to be the reason for the observed slow steady-state turnover of mutant G352V.

3.6. Mutant V380M

For mutant V380M the CO recombination kinetics were unchanged but the recombination of cyanide with the reduced enzyme occurred at only 15% of the wild-type rate (Table 3). The fast reaction of the reduced enzyme with oxygen (Table 5) demonstrated the functionality of the binuclear centre.

The E_m of haem *a* was not changed but a 65 mV higher E_m of Cu_B and a 85 mV more pronounced negative interaction between haem *a* and Cu_B was observed (Table 4). This observation was also evident from redox titrations of the unligated and formate-ligated enzyme (data not shown). Table 5

As for mutant G352V, the electrons from cytochrome *c* accumulated on haem *a* in the FIRE experiment at a rate too fast to account for the impaired turnover number, but again with markedly decreased transfer to the binuclear centre in comparison to the wild-type enzyme (Table 6). This observation contrasted with the measured equilibrium mid-

Table 6
Reduction of oxidised cytochrome *c* oxidase by ferrocytochrome *c*

	Parental	I67N	G352V	V380M
Observed rate of reduction of haem $a(s^{-1})$	22	22	22	18
Total ferrous *c* produced(μM)	0.64	0.75	0.68	0.5
Ferrous *c* after equilibration(μM)	0.12 (19%)	0.32 (43%)	0.23 (34%)	0.2 (40%)
Percentage of oxidase electrons on haem *a*	23%	11%	63%	51%
Percentage of oxidase electrons on binuclear centre	77%	89%	37%	49%

Photoreduction was carried out as described in Fig. 1 and analysed as described in the text.

point potentials in V380M, above, which indicated an elevated midpoint potential of Cu_B.

4. Discussion

4.1. A comprehensive approach to analyse cytochrome c oxidase mutants

A general aspect of this work has been the development of a comprehensive approach that can serve as a rationale to analyse functionally deficient mutants of cytochrome *c* oxidase independent of their source: The first step in this approach is to check for structural integrity of the isolated enzyme by analysing its subunit composition. Optical and EPR spectra were used to test for major structural changes and to give some first indications of which redox-centre might be affected by the amino acid exchange. The homogeneity of a cytochrome *c* oxidase preparation is best checked by monitoring cyanide binding to oxidised enzyme and carbon monoxide and cyanide recombination with reduced enzyme. By comparing the results for whole cells, mitochondrial membranes and isolated enzymes one can discriminate between preparation-induced and mutation-induced heterogeneity. The tests described allowed us to decide whether the functional changes we observed for a given mutation were due to specific localised effects, rather than due to poor assembly or general inhomogeneity of the enzymes in the preparation. In fact, one of the mutants tested here (T316K) did not meet our 'quality control' standards with respect to its homogeneity and was therefore omitted from further analysis (see Results). It is of particular importance to test the homogeneity of purified enzyme as cytochrome *c* oxidase is known to be amenable to modifications upon its isolation from mitochondrial membranes which, like the generation of 'slow reacting' oxidase [34,13,26], can cause artefactual results in subsequent functional studies. For the same reason we did not try to remove the remaining impurities in our enzyme preparations which were found not to be caused by incomplete assembly of cytochrome *c* oxidase and did not interfere with our experiments.

The second part of the approach was designed to efficiently pinpoint the functional defect caused by the mutation. The midpoint potentials of the different redox centres are determined to test for changes in their environment that affected this central thermodynamic parameter. The function of the binuclear-centre is tested by following the biphasic kinetics for the two transitions from the peroxy-form to the ferryl-form and from the ferryl-form to the oxidised form of the fully reduced enzyme reacting with oxygen. Ligand binding studies (see above) also provide additional information on the oxygen binding site. Finally, the electron entry side of the enzyme and the internal electron transfer is tested using the FIRE technique by following the distribution of a single electron entering the oxidised enzyme from cytochrome *c*.

4.2. Isolation of mutants to study the mechanism of cytochrome c oxidase by random mutagenesis

By using a selection strategy aimed at the isolation of non-functional but spectrally intact mutants from random mutagenesis of the yeast *Saccharomyces cerevisiae* [10] we isolated and analysed four mutations of the mitochondrially coded subunit I of cytochrome *c* oxidase. The usefulness of this approach becomes evident from the fact that three of the four mutations are in positions that have not been subjected to site-directed mutagenesis as their functional relevance could not easily be deduced even from the X-ray structure of subunit I. Moreover, all four mutations resulted in a more than 95% loss of steady state activity and had rather specific effects on distinct parts of the catalytic machinery. This is essential to obtain useful information from functionally deficient mutants at a level required for a more detailed understanding of the mechanism of cytochrome *c* oxidase.

Although high-resolutions structures are available for *P. denitrificans* and bovine heart cytochrome *c* oxidase [3,4], one would expect that much of this structural information can be used to rationalise the results obtained with mutants in *S. cerevisiae*, regarding the high degree of conservation between the amino acid sequences and structures of the bacterial and mitochondrial enzyme. The following discussion of the experimental results obtained with the yeast mutants studied here will specifically address this point. It will become obvious that, with few limitations, the *P. denitrificans* structure indeed can be used to obtain a detailed understanding of functional

mutations in the yeast enzyme. If necessary, mutations identified following random mutagenesis in yeast could be introduced into *Paracoccus* oxidase to analyse the structural changes involved in detail. Comparison of the structure of *Paracoccus* with the recently released structural coordinates of bovine heart oxidases revealed that all pertinent distances were the same in the surrounding of the investigated residues within the resolution of the two structures. Also, the additional proton channel proposed for the bovine heart enzyme by Tsukihara et al. [4] is located at the farnesyl edge of haem *a* and its protonable groups are more then 10 Å apart from all residues changed in the mutants under study here.

4.3. Mutant I67N

The analysis of the properties of cytochrome *c* oxidase isolated from mutant I67N presented here indicated that the changes induced by mutation I67N were strictly confined to the immediate environment of haem *a*. Visible and EPR spectroscopy revealed a moderate perturbation of the environment of this redox-centre and a shift of its midpoint potential by 54 mV to the negative, which explains the decreased reduction level of haem *a* in the FIRE experiment. The homologous residues in the *Paracoccus* and bovine sequence are M99 and I66, respectively, and are part of the irregular helix 2 of subunit I. This residues points towards the porphyrin ring of haem *a* and are located just below one of the histidine ligands of haem *a*. The closest distance between the sulfur atom of the methionine from *Paracoccus* and the porphyrine ring is 4 Å. This suggests that the observed spectral perturbations and the shift of the midpoint potential of haem *a* are likely due to the introduction of a more polar asparagine in the vicinity of the porphyrine ring.

However, the observed shift of the midpoint potential by itself is not sufficient to account for the low steady-state activity of enzyme from mutant I67N. A more detailed analysis of the structure around M99 revealed that the region of the protein around this residue is loosely packed. Thus, the difference between methionine and isoleucine within an otherwise highly conserved region of the protein is not expected to affect the local folding dramatically. Moreover, an isoleucine placed at position 99 largely overlaps with the original methionine and fits well into the structure of *Paracoccus* subunit I. From this and because of the very high degree of structural similarity between the published bacterial and mammalian structures, it seemed justified to simulate the mutation in the *Paracoccus* structure. This simulation revealed a possible interaction of the asparagine in position 99 with glutamic acid E278 (*Paracoccus* numbering) which corresponds to E243 in yeast and E242 in bovine subunit I. While the carboxyl group of E278 is about 5 Å apart from the sulfur of M99 the distance between the amide nitrogen and one of the oxygens of the carboxyl group was only 2.7 Å in one of the preferred rotamers of asparagine in position 99, which is a typical distance for the formation of an hydrogen bond. Although this observation has to be taken with great caution, it could be significant for the interpretation of the defect in mutant I67N: E278 represents a conserved charge within the membrane and has been proposed by Iwata et al. [3] to be part of one possible input channels for protons. If an additional hydrogen bond would exist in the mutant enzyme as suggested above, the primary reason for the low activity of the mutant enzyme could be that this proton channel was interrupted at E278. The functional importance of E278 has also been demonstrated by mutations of this residue to glutamine in *Rhodobacter sphaeroides* cytochrome *c* oxidase [25] and to alanine in cytochrome *bo* from *Escherichia coli* [24], both of which resulted in inactive enzyme. Further studies focusing on the effect of pH on the properties of the mutant enzyme are in progress to test whether the functional defect of mutant I67N is in fact due to an impairment of proton uptake and how this relates to the observed changes of the haem *a* environment.

4.4. Mutations near the binuclear centre

For the mutant G352V the rate of carbon monoxide rebinding and the dissociation constant for cyanide binding to the reduced enzyme were 30% of the wild-type rates. Also the reaction rate of the fully reduced enzyme with oxygen was only 50% of the wild-type rate. However, this rate was still too fast to attribute the slow steady state turnover of this mutant to its impaired ability to react with oxygen. Thus, the slow turnover number was rather due to the impairment of intramolecular electron transfer to the binu-

clear centre apparent from the accumulation of electrons on haem *a* in the FIRE experiment (cf. Table 6). No significant spectral changes were observed and none of the measured midpoint potentials for the redox centres was altered by mutation G352V. This indicated that no major changes of the environment of the prosthetic groups were induced by the mutation. We therefore propose that the poor equilibration of haem *a* with the binuclear centre may be due to an impairment of proton uptake into sites close to the binuclear centre. Such proton uptake is necessary in order to compensate the otherwise negative charges introduced by formation of the oxygen. This fits well with the position of the homologous glycine G387 in the *Paracoccus* structure (G352 in the bovine subunit). The distance between its C_α and the hydroxyfarnesyl sidechain of haem a_3 is like in the bovine structure only 3–4 Å to the closest carbon atom and only 6 Å to the hydroxyl group, which has been proposed to contribute to a second proton input channel [3]. G387 lies in a tightly packed region of the protein. Therefore, the G352V mutation is likely to cause a displacement of the hydroxyfarnesyl sidechain of haem a_3. This is in line with the fact that the binuclear centre became unstable during redox titration in the absence of cyanide and that respiratory competence is restored in a revertant containing alanine in this position [35].

Enzyme isolated from the mutant V380M (V415 in the *P. denitrificans* and V380 in the bovine sequence) exhibited a midpoint potential for Cu_B which was shifted by 55 mV to the positive and the redox interaction between haem *a* and Cu_B was more pronounced. Again this potential shift is unlikely in itself to account for the low activity of the mutant enzyme. Other properties of cytochrome *c* oxidase isolated from the mutant V380M were similar to those obtained for G352V: Some moderate effects on ligand binding were observed, but the primary reason for the low activity of the enzyme seemed to a difficulty in electron transfer from haem *a* to the binuclear centre, even although the midpoint potential of Cu_B has become even more favourable for such transfer. This might again arise from kinetic difficulties in transfer or binding of protons required for the charge compensation of the oxygen intermediates at the binuclear centre, an effect that would explain the FIRE data but which would not be evident in the slow timescales required for the redox titrations. This proposal might be in accord with the position of the homologous valine V415 in the *Paracoccus* structure. The residue, which is only two residues away from histidine H413, the axial ligand of haem a_3 [36], is only 3 Å (3.6 Å in bovine) apart from the vinyl group of haem a_3. Thus mutation V380M is expected to induce a distortion of the binuclear centre that could interfere with proton uptake into the binuclear centre.

Acknowledgements

We are grateful to Prof. H. Michel for providing access to structural details of *Paracoccus denitrificans* oxidase. We thank Prof. P.P. Slonimski for valuable discussions, Dr. W.R. Hagen for measuring the EPR spectra and Dr. G.C.M. Steffens for performing the metal analysis. We are indebted to PD Dr. H. Schägger for his support with the isolation of membrane proteins and electrophoretic techniques. The work was supported by a Fellowship of the Deutsche Forschungsgemeinschaft to C.O and a grant of the C.E.C.

References

[1] M. Saraste, L. Holm, M. Lübben, J. van der Oost, Biochem. Soc. Trans. 19 (1991) 608–612.
[2] B.M. Geier, H. Schägger, C. Ortwein, T.A. Link, W.R. Hagen, U. Brandt, G. von Jagow, Eur. J. Biochem. 227 (1995) 296–302.
[3] S. Iwata, C. Ostermeier, B. Ludwig, H. Michel, Nature 376 (1995) 660–669.
[4] T. Tsukihara, H. Aoyama, E. Yamashita, T. Tomizaki, H. Yamaguchi, K. Shinzawa-Itoh, R. Nakashima, R. Yaono, S. Yoshikawa, Science 272 (1996) 1136–1144.
[5] A.J. Pierik, W.R. Hagen, Eur. J. Biochem. 247 (1991) 3656–3661.
[6] A. Helenius, K. Simons, J. Biol. Chem. 247 (1972) 3656–3661.
[7] G.C.M. Steffens, R. Biewald, G. Buse, Eur. J. Biochem. 164 (1987) 295–300.
[8] T.A. Jones, J.Y. Zou, S.W. Cowan, M. Kjeldgaad, Acta Cryst. A 47 (1991) 110–119.
[9] B. Meunier, P. Lemarre, A.-M. Colson, Eur. J. Biochem. 213 (1993) 129–135.
[10] S. Brown, A.-M. Colson, B. Meunier, P.R. Rich, Eur. J. Biochem. 213 (1993) 137–145.

[11] H. Schägger, G. von Jagow, Anal. Biochem. 199 (1991) 223–231.
[12] H. Schägger, G. von Jagow, Anal. Biochem. 166 (1987) 368–379.
[13] U. Brandt, H. Schägger, G. von Jagow, Eur. J. Biochem. 182 (1989) 705–711.
[14] D.W. Marquardt, J. Soc. Ind. Appl. Math. 11 (1963) 431–441.
[15] S. Brown, J.N. Rumbley, A.J. Moody, J.W. Thomas, R.B. Gennis, P.R. Rich, Biochim. Biophys. Acta 1183 (1994) 521–532.
[16] R. Mitchell, P.R. Rich, Biochem. Soc. Trans. 22 (1994) 705–709.
[17] B.C. Hill, S. Marmor, Biochem. J. 279 (1991) 355–360.
[18] P.R. Rich, S.A. Madgwick, S. Brown, G. von Jagow, U. Brandt, Biochem. Soc. Trans. 19 (1991) 263S.
[19] P.R. Rich, A.E. Jeal, S.A. Madgwick, A.J. Moody, Biochim. Biophys. Acta 1018 (1990) 29–40.
[20] B. Meunier, S.A. Madgwick, E. Reil, W. Oettmeier, P.R. Rich, Biochemistry 34 (1995) 1076–1083.
[21] Q.H. Gibson, C. Greenwood, Biochem. J. 86 (1963) 541–554.
[22] A.J. Moody, U. Brandt, P.R. Rich, FEBS Lett. 293 (1991) 101–105.
[23] B.D. Price, M.D. Brand, Eur. J. Biochem. 132 (1983) 595.
[24] J.W. Thomas, A. Puustinen, J.O. Alben, R.B. Gennis, M. Wikström, Biochemistry 32 (1993) 10923–10928.
[25] D.M. Mitchell, R. Aasa, P. Ädelroth, P. Brzezinski, R.B. Gennis, B.G. Malmström, FEBS Lett. 374 (1995) 371–374.
[26] G.M. Baker, M. Noguchi, G. Palmer, J. Biol. Chem. 262 (1987) 595–604.
[27] A.J. Moody, P.R. Rich, Biochim. Biophys. Acta 1015 (1990) 205–215.
[28] G. Goodman, J. Biol. Chem. 259 (1984) 15094–150998.
[29] D.F. Blair, W.R. Ellis, H. Wang, H.B. Gray, S.I. Chan, J. Biol. Chem. 261 (1986) 11524–11537.
[30] P. Nicholls, J.M. Wrigglesworth, Ann. NY Acad. Sci. 550 (1988) 59–67.
[31] N. Kojima, G. Palmer, J. Biol. Chem. 258 (1983) 14908–14913.
[32] M. Oliveberg, P. Brzezinski, B.G. Malmström, Biochim. Biophys. Acta 977 (1989) 322–328.
[33] M. Oliveberg, B.G. Malmström, Biochemistry 31 (1992) 3560–3563.
[34] A.J. Moody, C.E. Cooper, P.R. Rich, Biochim. Biophys. Acta 1059 (1991) 189–207.
[35] B. Meunier, F. Coster, P. Lemarre, A.-M. Colson, FEBS Lett. 321 (1993) 159–162.
[36] M.W. Calhoun, J.W. Thomas, J.J. Hill, J.P. Hosler, J.P. Shapleigh, M.M.J. Tecklenburg, S. Ferguson-Miller, G.T. Babcock, J.O. Alben, R.B. Gennis, Biochemistry 32 (1993) 10905–10911.